	Experiment title: Dynamic distribution of liquid in fluidized granular matter and porous media: from mixing to oil extraction	**Experiment number**: LTP MA-800
Beamline: ID15A	**Date of experiment**: from: 27/01/2010 to 02/02/201 and 30/06/2010 to 06/07/2010	**Date of report**:
Shifts: 2 X 18	**Local contact(s)**: BT1: Mario Scheel / BT2: Marco Di Michiel	*Received at ESRF:*

Names and affiliations of applicants (* indicates experimentalists):

<u>Ralf Seemann</u>, Experimental Physics, Saarland University, Saarbrücken, Germany and MPI for Dynamics and Self-Organization, Göttingen, Germany

<u>Stephan Herminghaus</u>, MPI for Dynamics and Self-Organization, Göttingen, Germany

<u>Martin Brinkmann</u>, MPI for Dynamics and Self-Organization, Göttingen, Germany

<u>Eckart Meiburg</u>, Mechanical Engineering Dep. University of California in Santa Barbara

<u>Marco Di Michiel</u>, E.S.R.F., Grenoble, France

Report:

In the framework of the long term proposal we study several aspects of wet model granulates which consist of spherical beads. The two main aspects are the forced imbibition of water into an oil filled bead pack as a model porous matrix to clarify the forced multiphase flow on a pore scale level. And we trace the position of individual particles in a fluidized bed of wet granulates to understand their dynamic behaviour. Consequently the report is divided in a first part on the multiphase flow and a second part on the particle dynamic.

Multiphase flow in porous media:

Understanding the dynamic behaviour of multiphase fluid flow in porous media has many applications, such as oil recovery from reservoirs, and remediation of oil contaminated soil by water/surfactant flood. There is still no deep understanding on the pore size level of how the advancing water-oil front behaves during water imbibition in initially oil saturated porous media at pore scale, and what factors leads towards fingering and by-passing of several oil filled pore pockets, therefore resulting in significant trapping of oil in porous media. This limited pore-scale knowledge is partly due to experimental difficulties associated with capturing high speed three-dimensional images with high spatial resolution. Developing a thorough physical understanding of multiphase fluid flow mechanisms at pore level would lead us designing effective recovery processes, and developing advanced models.

In the framework of our LTP at ID-15A, we studied the flow behaviour of a water flood in oil saturated artificial porous media. We constructed and tested a sample cell that allows for well controlled starting conditions for both a wettable and a non-wettable matrix and developed a suitable experimental procedure. The sample consisted of piles of glass/basalt beads, of diameter in the range 355-425 µm, packed in a cylindrical polycarbonate cell. The pile of glass beads are an example for a water wet system whereas the pile of basalt beads is an example for an oil wet system. The internal wall of the container was coated with a rubber layer (polydimethylsiloxane, PDMS). To inject the aqueous phase into the sample cell with reproducible and homogeneous start conditions we use an appropriately designed inlet which is covered by a

water wetting filter paper which separated the beads from the injection part. This sample design works both for water wet and oil wet sphere packs. A schematic of the sample cell is shown in fig. 1. Such prepared sample cells were first filled with oil, and then the beads were poured from the top; this procedure helped us to avoid air entrapment during filling. To guarantee that trapped air bubbles can be easily identified we did several experiments where the X-ray absorption of the oily phase was also increased by mixing it with e.g bromododecane [17 vol%].
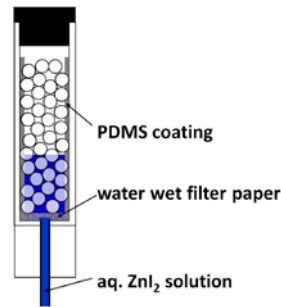
Figure 1: Schematic of the sample cell design. A water wet filter paper homogenizes the injected liquid front to enable homogeneous flooding over the cross section of the sample and a soft and hydrophobic rubber (PDMS) coating of the container walls prevents undesired imbibition at the container walls.

To conduct imbibition experiment the prepared sample cell was flushed with ZnI_2 solution from the base of the cell at a constant flow rate controlled by a computer controlled syringe pump. ZnI_2 solution was used as aqueous phase to enhance the X-ray contrast of water for clear distinction between aqueous phase and oil. The cell was imaged before and during aqueous phase flood using monochromatic beam which allowed time-resolved imaging with a voxel size of 18 µm (512 x 512 pixel) using the Sarnoff camera which was sufficient to resolve various phases at pore-scale of the chosen bead diameter. Similar experiments were conducted for different beads to alter the wettability of porous matrix, and for different flow rates.

The tomographic data were reconstructed and pre-processed to enhance image quality to allow for quantitative analysis at the pore scale. The pre-processing steps include noise reduction filtration (fig. 2a) and the application of geometric mask for outer cell removal (Fig. 2b). For phase segmentation, the segmented image containing only beads (fig. 2c) was applied as a mask on the rest of the images, to remove beads. This allowed an effective phase identification of a large number of tomographic datasets containing three different phases. Figure 2d shows a raw image with three phases, and fig. 2e shows the same image after segmentation using above mentioned procedure.
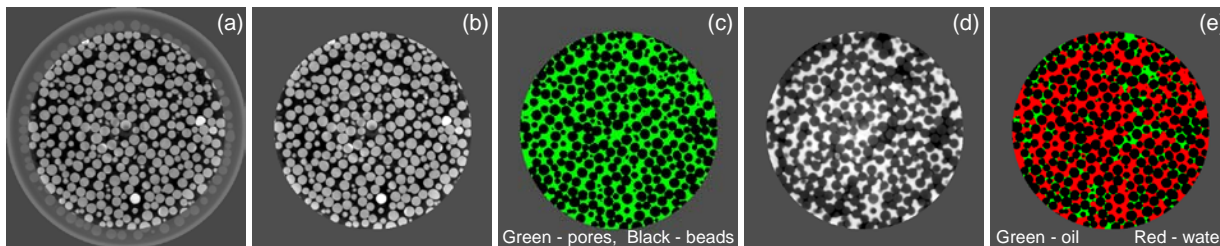

Figure 2: Schematic of some of the applied image processing steps: (a) anisotropic diffusion filtration; (b) application of geometric mask (to remove outer cell); (c) beads segmentation (black) to use as mask; (d) raw image with three phases after geometric mask; and (e) application of masked image (c) to subtract beads and segment water and oil in (d).

The masked image (fig.2c) was further processed to obtain network data which provided us pore and throat parameters, including pore and throat equivalent volume, pore and throat radius and throat length. The pore parameters were compared for glass and basalt beads, as shown in Figure 3. The porosity of glass and basalt samples was found to be approximately 38.3%. These pore parameters will be used to develop pore scale models.
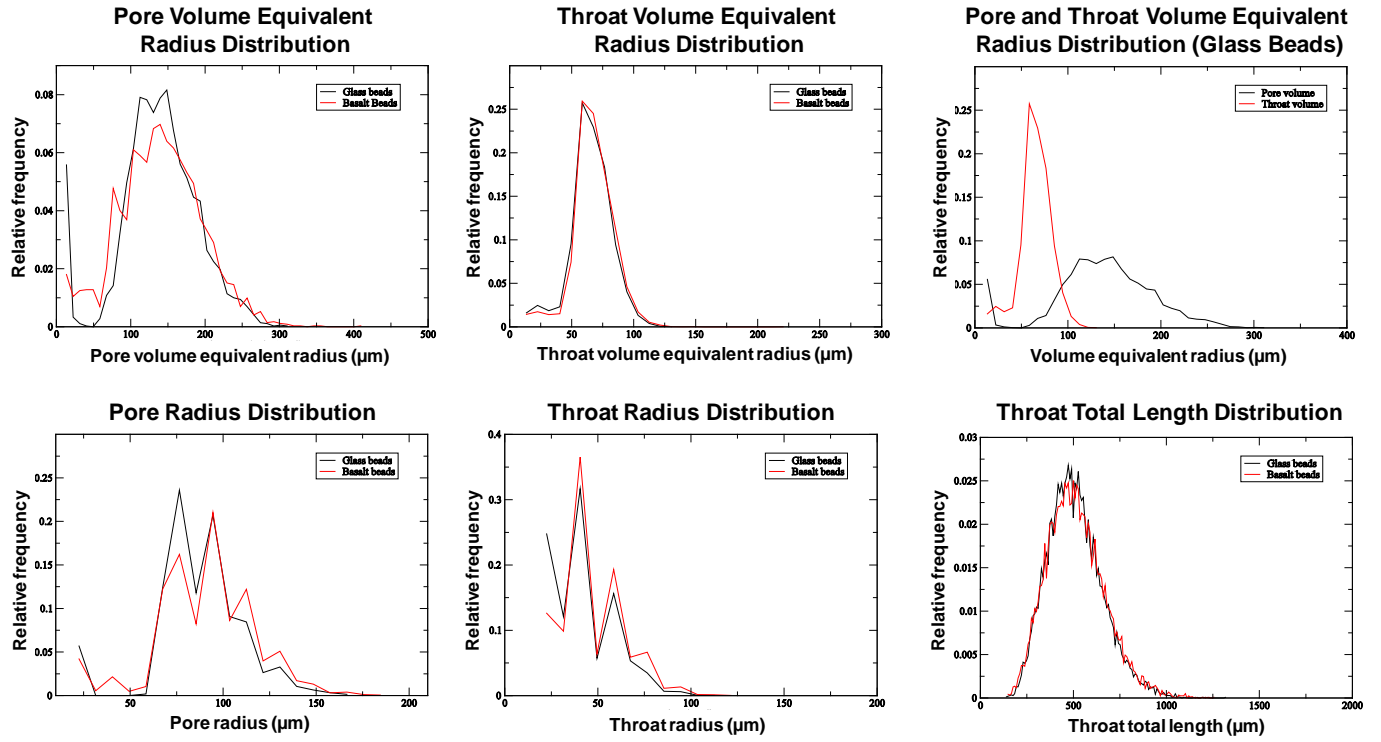
Figure 3: Pore and throat characterization of glass and bead matrices. In these figures, equivalent blob diameter corresponds to the diameter of a hypothetical sphere having the same volume as the actual blob.

Figure 4 (top row) shows two-dimensional slices of various time steps of glass bead experiments, where the aqueous phase (white) invades the oil filled glass beads (grey) from the base of the cell. The lower row shows the same time steps rendered in three dimensions. Here only water is rendered to observe the interface evolution with time. In these images, we can clearly observe the formation of aqueous phase fingers ahead of the overall water-oil front which ultimately result in by-passing of significant amount of oil which remains in position due to strong interfacial forces.
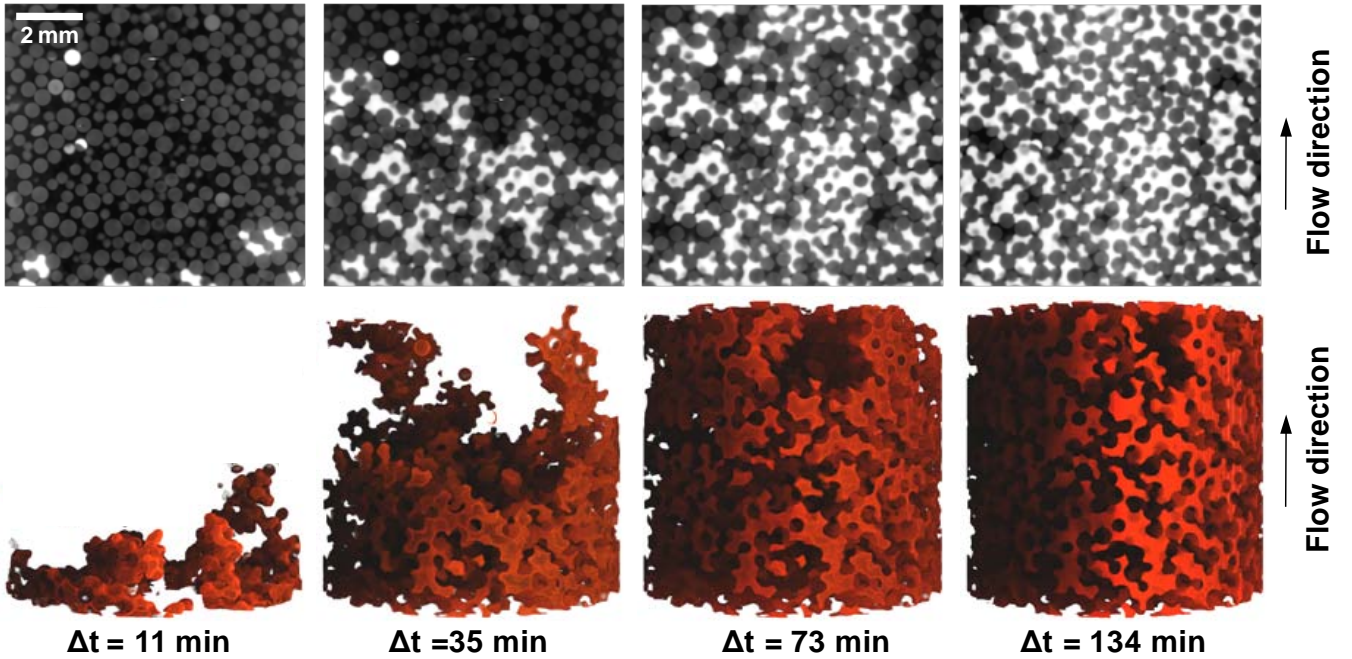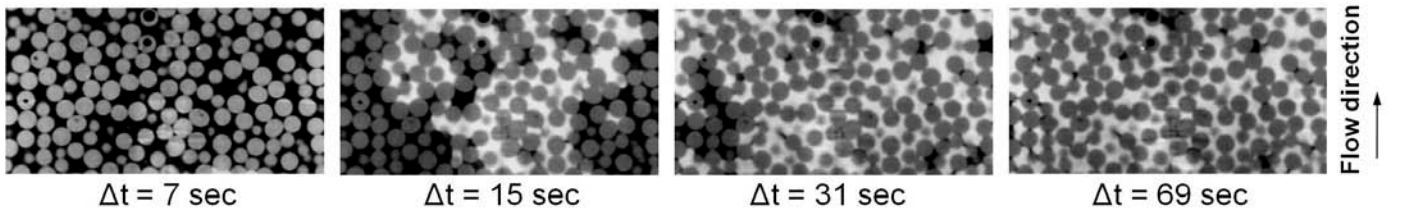

Figure 4: A time-series of water imbibition in glass-bead matrix initially filled with oil; the average front velocity is about 1 µm/s. The upper row shows the 2D slices of grey scale image at different time steps during aqueous phase (white) imbibition in oil (black) filled glass beads (grey). The lower row shows the same time steps rendered only for water in three dimensions.

Figure 5 shows the same type of experimental results but for an aqueous phase displacing an oil filled matrix of basalt beads with the same front velocity of about 1 µm/s and fig. 6 shows a liquid displacement experiment in basalt beads with an average front velocity of about 10 µm/s.

Δt = 0 min   **Δt = 12 min**   **Δt = 81 min**   **Δt = 139 min**
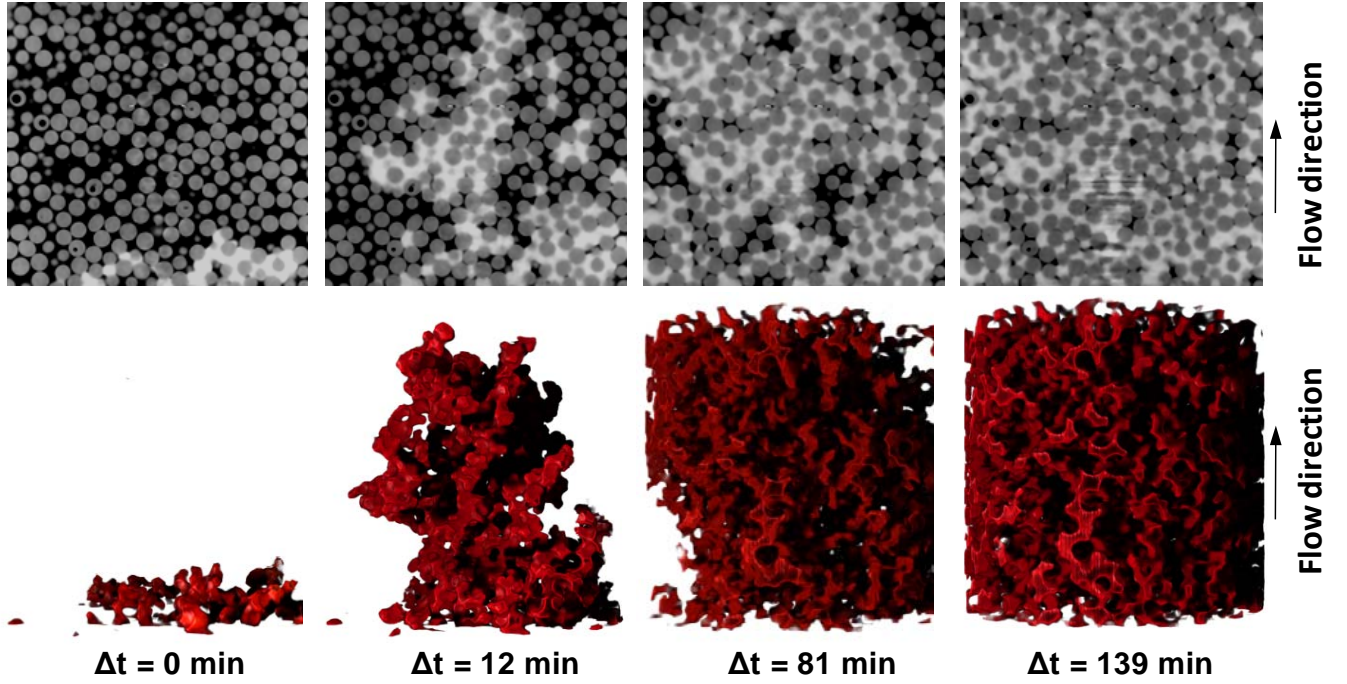
Figure 5: A time-series of water imbibition in basalt-bead matrix initially filled with oil; the average front velocity is about 1 µm/s. The upper row shows the 2D slices of grey scale image at different time steps during aqueous phase (white) imbibition in oil (black) filled glass beads (grey). The lower row shows the same time steps rendered only for water in three dimensions.

Δt = 7 sec   Δt = 15 sec   Δt = 31 sec   Δt = 69 sec

Figure 6: Time-series of water imbibition in basalt-bead matrix initially filled with oil. 2D slices of gray scale image are shown at different time steps during aqueous phase (white) imbibition in oil (black) filled basalt beads (grey). *Top row:* the average front velocity is about 1 µm/s. *Bottom row:* the average front velocity is about 10 µm/s.

The liquid fronts in the glass and basalt packs seem to be different. It seems that the front in the water wet glass system has more fingers whereas the liquid front in the oil wet basalt pile seems to be more compact. Unfortunately this is very difficult to display both as a cross section and as a 3d rendering. It will be one of the main goals for the future to develop means to quantitatively describe the front shape and front behaviour as a function of time. In first and crude attempts we preliminary analyzed the front length and the oil saturation as a function of time. But even in this analysis there is no clear distinction between the liquid front in glass and basalt bead packs. The likely reason for that is that both data sets are still dominated by contributions from the container wall which are not yet properly separated from the signal of interest.

A preliminary analysis of the change in oil saturation with time for glass and basalt beads are shown in fig. 7 for a slow flow rate of 1 µm/s (left) and fast flow rate of 10 µm/s (right). We also calculate the change in aqueous phase surface area with time. For all these analysis we have to develop appropriate means to account

for undesired effects at the side wall of the container which might influence the result in the quantitative analysis. We further analyse the size and shape of different oil clusters at residual saturation conditions.
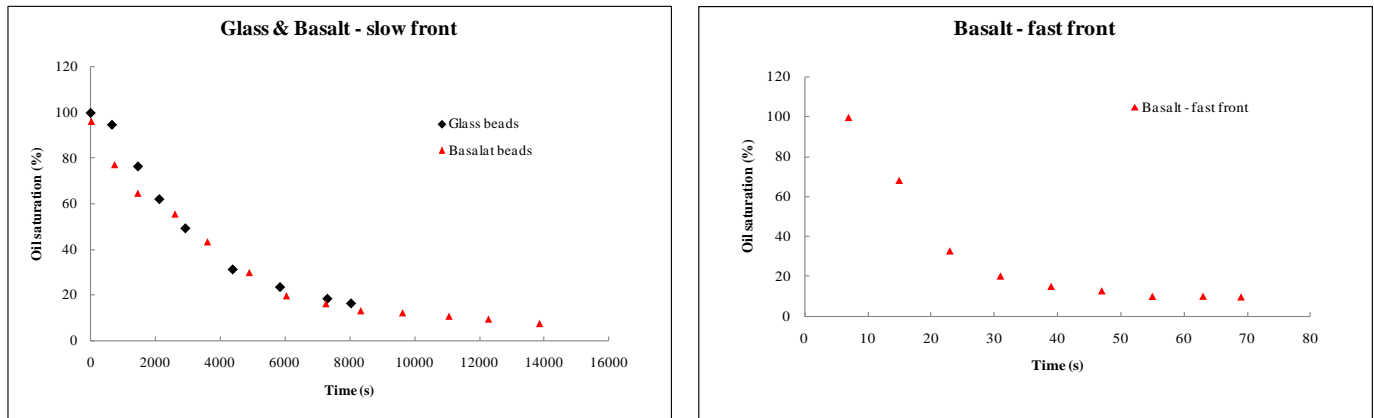
*Figure 7: **Oil saturation as function in time for glass (black symbols) and basalt beads (red symbols) in the case of a average flow rate of about 1 µm/s (left) and fast flow rates of about 10 µm/s (right).***

First and preliminary analysis of the data revealed that the data quality is sufficient for a quantitative analysis but more of the required image analysis steps should be explored to be able to automate the very time consuming processes and to allow for faster analysis and comparison of the 3d data. Furthermore an increased pixel resolution using the PCO Dimax camera would make the analysis easier and more precise and would be thus very welcome.

With our developed sample preparation method and experimental routine we typically imaged water/oil fronts with an average velocity of about 1 µm/sec at a data acquisition time of about 1-2 s and could go up to average front velocities of 10 µm/sec at 18 µm voxel resolution. We followed the front for more than two hours without any X-ray damage until no changes in the remaining oil were visible and captured between 200 and 400 tomography images during that time. To be able to image significantly smaller beads respectively pore sizes at similar imaging speed several technical developments are in preparation: we expect to use a new 2x optics with larger aperture which shall be available soon and should allow to capture full tomography images at presumable 2-3 s acquisition time and a resolution of 9 µm using the current camera (Sarnoff). The implementation of a new camera (PCO Dimax) is in progress and should allow for 11 µm resolution using a 1x optic at 1 k x 1 k pixels and a resolution of 5.5 µm using the 2x optics at 2 k x 2 k pixels. The assumed imaging time for the 5.5 µm resolution is expected to be around 10 s if all parameters are optimized.

Dynamics of a fluidized wet granulate

It is intuitively clear that adding fluid to dry grains alters their mechanical properties; every child knows that the properties of a sand pile change dramatically when the sand is wet, and that the resulting stiffening can be exploited to construct sandcastles. When a small amount of fluid is added to dry grains, the fluid will form bridges at the grains' contact points. The surface energy of the liquid bridges results in the presence of an attractive force between grains in contact which is absent in dry granulates; therefore, wetting changes the medium from one with only repulsive interactions between the grains to one with both repulsive and attractive interactions [1-3]. Given that the microscopic physical interactions between the grains are fundamentally different for wet grains, it is not plausible to directly apply the existing knowledge base developed for dry systems to wet ones. The presence of a wetting liquid in the sample poses an additional challenge; the granular sample is not optically transparent and standard techniques for determining the three dimensional flow of grains (stereo PIV or PTV) can no longer be applied.

In our experiments we probed the three-dimensional flow of tracer particles embedded in fluidized grains using a new technique; high speed synchrotron X-ray stereoscopic particle tracking [4]. X-ray radiation from the undulator source (U22) at ID 15 was monochromatized by two bent Laue (111) silicon crystal monochromators. The single beam was split into two beams of equal intensity using a bent Laue monochromator which reflected approximately half of the incident photons at an angle $\alpha = 2\theta = 4.236^\circ \pm 0.002^\circ$ (where θ is the Bragg angle), and transmitted the other half as sketched in fig. 8a. The sample was placed in the region where the two beams overlap and was imaged using a single detector, a high speed camera. The camera was positioned to be perpendicular to the direct beam at a sufficient distance such that the two beams did not overlap. With this setup, the camera simultaneously recorded two images of the sample taken from two views separated by an angle α, thus the deflected beam was projected with the angle α onto the detector. Making use of the large flux generated by the undulator source, we were able to use exposure times of 1 ms to simultaneously obtain the stereo absorption images.
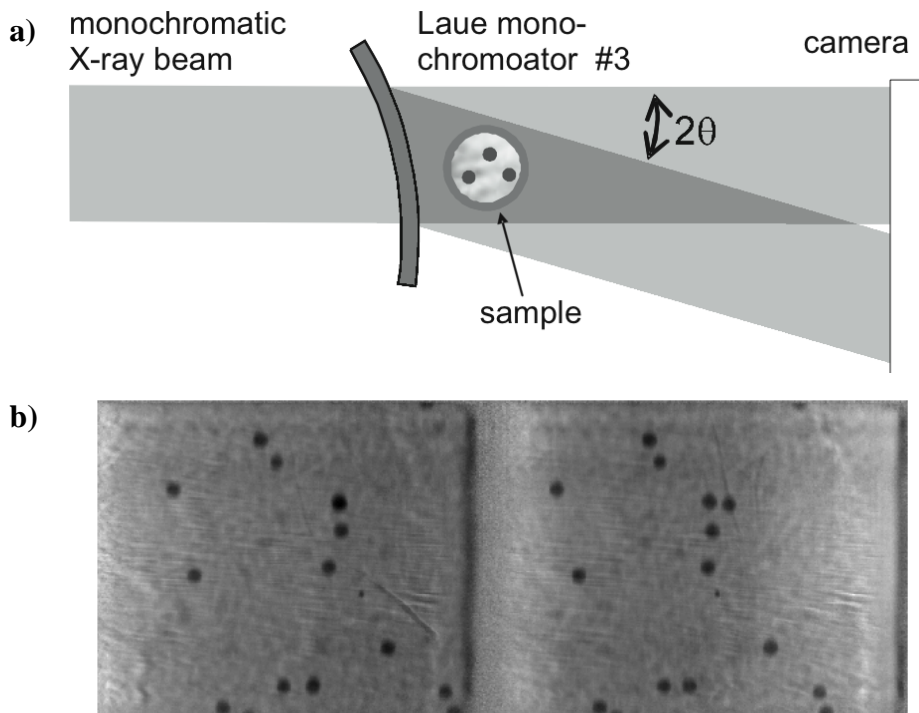
Figure 8: *a)* Sketch _____ving the two projected absorption images (left: reflected beam and right: direct beam) from different view angles on the chip of a single camera. The granular sample consisted of glass spheres (background) seeded with BaTi tracer particles (darker round objects) agitated at 100 Hz with a peak acceleration of 5.4 g (1 g = 9.8 m/s^2) and a wetting content of 0.01% by volume. There are some unexposed pixels at the right edge and center of the image.

Our granular samples consisted of glass beads fluidized by an electromagnetic shaker; we agitated the samples continuously while obtaining fast stereo x-ray absorption images. Our samples consisted of glass spheres with diameters in the range of 300-355 mm and the tracers were highly absorbing BaTi tracer

particles with the same range of sizes. The combination of these two materials have a sufficiently large x-ray absorption contrast to allow for a clear distinction between the tracers and surrounding media in each absorption image. Silicone oil was used as the wetting liquid in these experiments since its' boiling point is above 250 °C, and it does not suffer from radiation damage. In our experiments we varied the wetting content of the samples while keeping the vibration acceleration and frequency fixed in order to examine the effects of varying wetting content on the grain dynamics. The sample was filled to a height of 25 mm, and the center of the sample was imaged stroboscopically with the sample's vibration frequency in order to measure the resulting tracer trajectories. Figure 8b shows an image of a sample obtained from a split beam.

From raw images such as those shown in fig. 8b, we are able to determine the three dimensional position of the tracer particles using geometric ray tracing [4]. An example of reconstructed 3D trajectories of selected tracer particles, embedded in our sample described above, is shown in fig. 9a. Fine-scale details of the tracers' motion are well resolved, as the close-up view shown in fig. 9b demonstrates. Using time resolved fully 3d position data such as has been shown here, we can probe the transport properties and material stiffness of fluidized wet granular materials, eg. using passive tracer microrheology techniques [5].
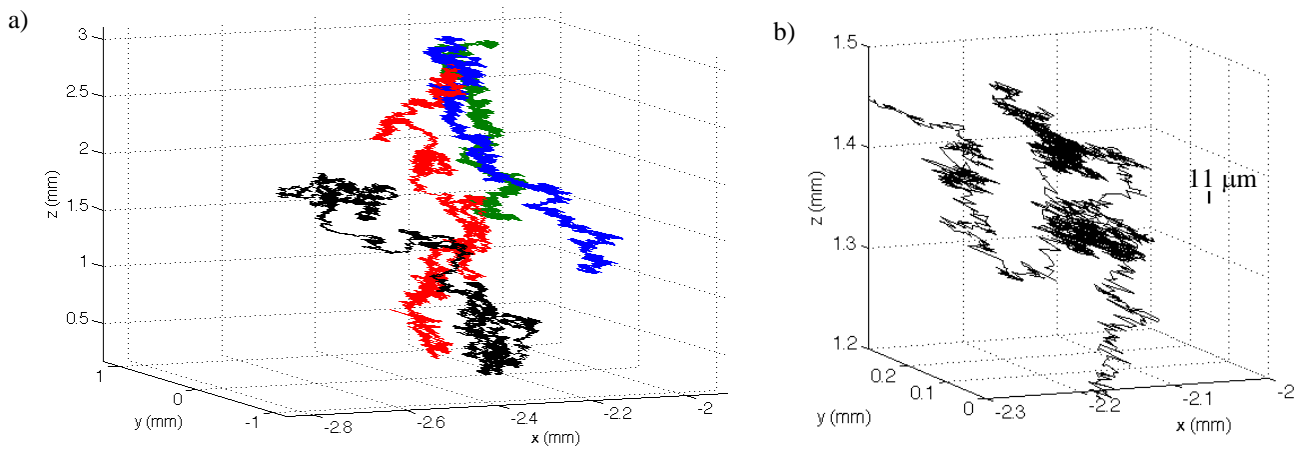
Figure 9: a) 3D reconstructed trajectories of BaTi tracer particles embedded in a fluidized sample of 300-355 mm spheres vibrated with a frequency of 100 Hz and, a peak acceleration of 5.4 g and a wetting content of 0.01%. *b)* Close-up view of a single trajectory from a).

References

1. H. M. Jaeger, S. R. Nagel, and R. P. Behringer, *Rev. Mod. Phys.* **68**, 1259 (1996).
2. T. C. Halsey and A. J. Levine, *Phys. Rev. Lett.* **80**, 3141 (1998).
3. M. Scheel, R. Seemann, M. Brinkmann, M. Di Michiel, A. Sheppard, B. Breidenbach and S. Herminghaus, *Nature Materials* **7**, 189 (2008).
4. M. DiMichiel, Z. S. Khan, M. Scheel and R. Seemann, in preparation.
5. J. C. Crocker, M. T. Valentine, E. R. Weeks, T. Gisler, P. D. Kaplan, A. G. Yodh, and D. A. Weitz, *Phys. Rev. Lett.* **85**, 888 (2000).

Two almost finished manuscripts, one in preparation, see supplement